

Robust, gapped, flat bands at half-filling in the minimal model of the superconducting metal-organic framework, Cu-BHT

M. F. Ohlrich,^{1,*} H. L. Nourse,² and B. J. Powell¹

¹*School of Mathematics and Physics, The University of Queensland, 4072, Australia*

²*Quantum Information Science and Technology Unit,*

Okinawa Institute of Science and Technology Graduate University, Onna-son, Okinawa 904-0495, Japan

The superconducting metal-organic framework Cu-BHT forms a kagome lattice with metals at the vertices and ligands along the bonds. We show that a tight-binding model with metal and ligand sites on this lattice yields five flat topological bands (FTBs), three of which are partially occupied at half-filling, with large gaps between them and all other bands. Long-range hopping induces curvature in the FTBs but leaves them flatter and more isolated than those in twisted bilayer graphene. Thus, framework materials are ideal materials for exploring flat band physics at high electronic densities.

Flat bands, where the energy of the electrons is independent of their momentum [1, 2], were brought to the world stage by the discovery of superconductivity and strongly correlated insulating states in twisted bilayer graphene (TBG) [3, 4]. These phenomena are found at the ‘magic angle’, $\sim 1.1^\circ$, where the moire pattern leads to a group of isolated, narrow bands (often called ‘nearly flat bands’), with a total bandwidth on the order of 10 meV, and band gaps of the same order on either side [3, 5]. This led to suggestions that superconductivity in TBG may be linked to the strong electronic correlations in the nearly flat bands [1].

Understanding superconductivity in strongly correlated electron systems is one of the grand challenges of modern physics. Superconductivity is found near correlated insulating phases in the cuprates [6], organic superconductors [7], Na_xCoO_2 [8, 9], Sr_2RuO_4 [10], iron pnictides [11] and some heavy fermion materials [12].

Many correlated insulating states occur in metal-organic frameworks (MOFs), coordination polymers (CPs) and covalent organic frameworks (COFs) [13–20]. Therefore, these systems are excellent candidates to display unconventional superconductivity when driven out of their insulating phases, e.g., by doping [21], pressure, or control of chemistry [22]. This hypothesis received strong support from the recent discovery of superconductivity in copper(II) benzenehexathiolate (Cu-BHT) [23], and from the clear evidence for unconventional superconductivity and strong electronic correlations in this material [24].

In this Letter, we study the simplest possible model of Cu-BHT: a tight-binding model on a lattice that is to the kagome lattice as the Lieb lattice is to the square lattice (henceforth the kagome-Lieb lattice; Fig. 1a). At half-filling, the five bands nearest the Fermi energy are flat and three of these flat bands lie at the Fermi energy, Fig. 1b. We give a simple explanation for these flat bands in terms of the lattice topology. We show that, and

explain why, they are robust to the largest expected perturbations (orbital energy differences between the metals and ligands and direct metal-metal hopping). Even when longer-range hopping is introduced, which induces some curvature, the three bands nearest the Fermi energy remain narrower and more isolated than the nearly flat bands in TBG.

Understanding flat band systems is of general interest beyond TBG: in a flat band, the kinetic energy of all electrons is equal and the behavior of the system is determined by the electronic interactions. In a nutshell, strongly correlated phenomena are amplified by flat bands. Thus, flat band systems are playgrounds for exotic phenomena, such as the fractional quantum Hall effect, high temperature superconductivity, and metal-insulator transitions [1, 2]. TBG has an extremely low electron density, but many of the most interesting predictions for flat bands require high electron densities [1, 25]. Additional characterization techniques are available in bulk materials that cannot be used in moire systems. Thus, discovering bulk materials with flat bands is an important goal, for which CPs, MOFs, and COFs offer unique advantages.

CPs are highly tunable materials, which consist of metallic centers bonded to organic groups (ligands) [26]. These ligands link to other metals to form a crystal. Advances in coordination chemistry allow for ‘crystal engineering’ [27, 28]: the rational design of crystal structures [26–29]. Thus, realizing specific lattice structures in CPs is a highly achievable objective. MOFs are the subclass of highly porous CPs [30], with widespread potential applications, such as carbon capture and storage, hydrogen fuel storage, microelectronics, and drug delivery [13, 14, 30]. COFs are similar to CPs and MOFs, but with the metals replaced with another organic group [15, 31]. Again, COFs offer exquisite control of structural and electronic properties [32].

In many CPs and MOFs, including Cu-BHT [23, 24], the metals form a kagome lattice with the ligands lying along the nearest neighbor bonds [33–35]. For example, in Cu-BHT, density functional theory (DFT) shows that the low-energy electronic structure is dominated by

* miriam.ohlrich@uq.net.au

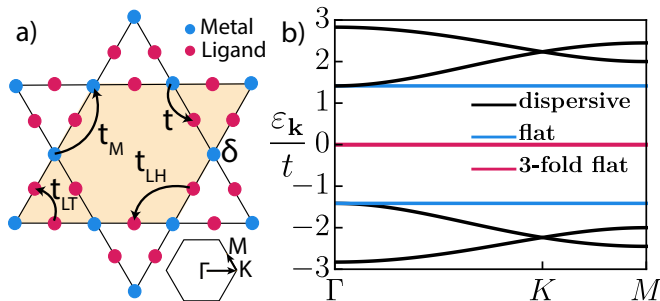


Fig. 1. Tight-binding model on the kagome-Lieb lattice. (a) Hopping integrals are marked, δ is the site energy of the metals, and the shaded area is the unit cell. The Bravais lattice is inset; Γ , M and K label the high symmetry points. (b) Band structure of the nearest neighbor model.

bands that originate from the Cu and S atoms with little weight on the C atoms [22]; structurally, the S atoms sit along the nearest neighbor Cu-Cu bonds. As both the metals and ligands have orbitals near the Fermi energy, the simplest possible model is the tight-binding model on the kagome-Lieb lattice, Fig. 1a. Indeed, increasing covalency between metals and ligands is a design strategy for achieving metallic and superconducting MOFs [13], which motivated the first studies of Cu-BHT [24], and necessitates electronic models including both the metals and the ligands. This lattice also occurs quite naturally in COFs [31]. In contrast, the kagome-Lieb lattice structure is absent from a recent catalog of flat-band inorganic materials [25].

We study the Hamiltonian

$$H = - \sum_{\alpha, \sigma} \sum_{\langle i, j \rangle_{\alpha}} t_{\alpha} \hat{c}_{i\sigma}^{\dagger} \hat{c}_{j\sigma} + \delta \sum_{i \in M, \sigma} \hat{c}_{i\sigma}^{\dagger} \hat{c}_{i\sigma}, \quad (1)$$

where $\hat{c}_{i\sigma}^{(\dagger)}$ creates (annihilates) an electron of spin σ in an orbital at site i , the sum over $i \in M$ includes metal sites only, and $t_{\alpha} \in \{t, t_M, t_{LH}, t_{LT}\}$ are the hopping amplitudes sketched in Fig. 1a. Although there are nine sites per unit cell, we were able to solve this model analytically.

It is helpful to first understand the nearest neighbor model ($\delta = t_M = t_{LH} = t_{LT} = 0$). At half-filling, the five bands nearest the Fermi energy are flat. This includes three degenerate flat bands which are found at the Fermi energy and two ‘kagome-like’ flat bands: flat bands that touch two dispersive bands, which also resemble the bands of the kagome lattice (Fig. 1b).

Sutherland’s theorem [36] states that for any bipartite tight-binding model there are at least $N_A - N_B$ degenerate flat bands, where $N_A = 6$ is the number of sites per unit cell on the A sublattice (ligands), and $N_B = 3$ is the number of sites per unit cell on the B sublattice (metals). Furthermore, Sutherland’s theorem requires that the energy of these bands equals the Fermi energy of the half-filled system. Thus, the three degenerate flat bands on the kagome-Lieb lattice is the smallest number compati-

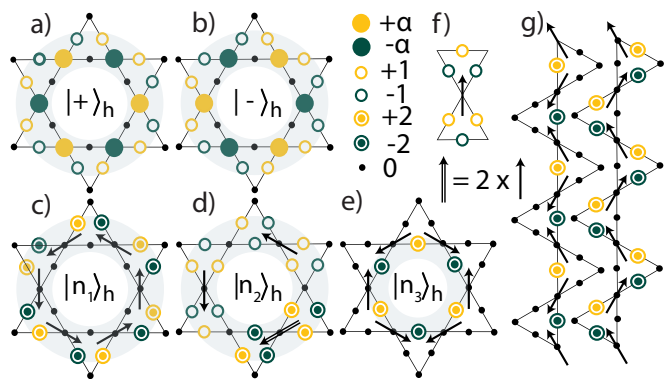


Fig. 2. (Unnormalized) localized eigenstates for each of the flat topological bands. Electrons cannot hop outside the loops due to destructive interference. The (a) antibonding ($|+\rangle_h$) and (b) bonding ($|-\rangle_h$) kagome-like eigenstates have energies $E_{\pm} = [t_{LT} + 2t_M + \delta \pm \sqrt{8t^2 + (2t_M - t_{LT} + \delta)^2}]/2$ and a relative amplitude on the metal sites of $\alpha_{\pm} = (E_{\pm} - t_{LT})/t$ (for $t_{LH} = 0$). The three non-bonding (between metals and ligands) eigenstates (c-e) can be constructed as superpositions of bow-tie states (f), as can noncontactable loops for PBC (g). The superpositions are indicated by the arrows which define the sign of the bow-tie wavefunctions centered on each metal site.

ble with Sutherland’s theorem. However, the kagome-like flat bands are not required by Sutherland’s theorem.

Flat bands correspond to localized states. These can emerge trivially, when the hopping amplitudes vanish, or topologically, due to quantum interference [2, 37–39]. The analytical expressions for the localized wavefunctions (Fig. 2) of the kagome-Lieb tight-binding model reveal that these are flat topological bands (FTBs). The localized wavefunctions for three degenerate FTBs only contain weight on ligands. However, the two kagome-like FTBs also include support on the metals, with relative amplitude $\pm\alpha$; for the nearest-neighbor model, $\alpha = \sqrt{2}$.

The localization of these five FTBs can be readily understood from the topology of the lattice. For each wavefunction, the sites with zero amplitude are either nearest neighbors of only sites with zero amplitude, or nearest neighbors of two such sites with opposite phases and equal magnitudes, leading to destructive interference when the Hamiltonian acts on the wavefunction. Thus, the localized states are eigenstates.

The localized states that comprise the flat-band of the kagome lattice consist of alternating sign amplitudes around each hexagon [37]. The kagome-like FTBs on the kagome-Lieb lattice are composed of the (anti)bonding combination of the metals and two nearest neighbor ligands on hexagon h . These hybrid orbitals form flat band states, ($|+\rangle_h$) $|-\rangle_h$, analogous to those found in the kagome lattice. The dispersive bands with (high) low energies are also kagome bands in the basis of the (anti)bonding states of metals/nearest neighbor ligands. This explains the Dirac points at K and K' (Fig. 1b). In contrast, the three degenerate FTBs are non-bonding

(between metals and ligands), as they have no weight on the metal sites (Fig. 2c-e). The non-bonding states can also be understood as superpositions of ‘bow-tie’ states, centered on a metal, although the state has zero amplitude on the metal, Fig. 2f.

The two kagome-like flat bands touch a dispersive band at the Γ point ($k = 0$). This has a simple explanation, analogous to that for the kagome [37] and other decorated kagome lattices [39]. Each unit cell contains one hexagon (Fig. 1). Therefore, for N unit cells and open boundary conditions (OBC) there are N (anti)bonding kagome-like FTB states. Superpositions of $|\pm\rangle_h$ states on adjacent hexagons have zero weight on the sites that contribute to both localized wavefunctions due to destructive interference. Therefore, $\sum_h |+\rangle_h = \sum_h |-\rangle_h = 0$ for periodic boundary conditions (PBC), leaving $N - 1$ non-trivial superpositions of $|+\rangle_h$ ($|-\rangle_h$). However, for PBC one can construct two additional states, which cannot be written as superpositions of $|+\rangle_h$ ($|-\rangle_h$), and wrap around the lattice (i.e., one noncontractable composed of (anti)bonding states in each of the x and y directions) [37, 39]; resulting in $N + 1$ states with energy E_{\pm} . As each FTB can only accommodate N states, topology dictates that cannot be a gap between the kagome-like FTBs and the dispersive bands.

The non-bonding states are most easily counted in the basis of bow-tie states (Fig. 2f). There are three metal sites, and thus three bow-tie states, per unit cell. No non-trivial superposition of the bow-ties vanishes. All noncontractable loops are superpositions of bow-ties (Fig. 2g). Thus, there are $3N$ bow-tie states for either OBC or PBC and topology does not require that the three non-bonding FTBs touch other bands.

The absence of topologically required band touching for the non-bonding FTBs has a profound consequence: it allows significant gaps between the non-bonding FTBs and the dispersive bands. In contrast, the FTBs on the kagome [37], Lieb [38], pyrochlore [37], and star [39] lattices all have topologically required band touchings and therefore excitations into dispersive bands at arbitrarily low energies. Thus, materials realizing these lattices are significantly less promising candidates to explore flat band physics at high electronic densities than materials that form kagome-Lieb lattices.

As of yet, we have only considered the simplest possible tight-binding model. It is unlikely that this simple Hamiltonian will be realized in any material (although it may be possible for ultracold gases in optical lattices). The most important correction will commonly be a mismatch in the orbital energies of the metals and ligands. This energy difference is described by an on-site potential for the metals, δ [Eq. (1)]. Non-zero δ does not induce a curvature in the FTBs regardless of its magnitude. We can understand this in terms of the localized wavefunctions sketched in Fig. 2. The lattice is bipartite for any value of δ , therefore, the three degenerate bands are guaranteed to remain flat for all δ . However, we can see this more intuitively because none of the localized

wavefunctions contain any amplitude on the metal sites, Fig. 2c-e, which is also a consequence of Sutherland’s argument [36]. The two kagome-like FTBs (and the four kagome-like dispersive bands) remain, as δ simply renormalizes the amplitudes on the metal and ligand orbitals in the (anti)bonding orbitals that form the natural basis for these bands.

Positive δ increases the energy gap between the non-bonding FTBs and the three bonding kagome-like bands, Δ_h ; it also decreases the energy gap between the three anti-bonding kagome-like bands and the degenerate bands, Δ_e , but much less. These trends are reversed for negative δ , as $\delta \neq 0$ breaks particle-hole symmetry. Non-zero δ also narrows all of the dispersive bands, Fig. 3a.

Direct metal-metal hopping, t_M , does not cause any of the five FTBs of the kagome-Lieb lattice to become dispersive, Fig. 3b. This is surprising as the lattice is no longer bipartite for $t_M \neq 0$. Therefore, Sutherland’s theorem no longer guarantees that the model retains the three non-bonding FTBs. However, the non-bonding FTBs have zero amplitude on all metal sites; therefore metal-metal hopping cannot perturb them. The two kagome-like FTBs have non-zero amplitudes on the metal sites. However, in $|+\rangle_h$ and $|-\rangle_h$, the phases of the metal sites alternate around each hexagon and are therefore localized by destructive interference under direct metal-metal hopping, Fig. 2. Therefore, the contribution to the energy of kagome-like FTBs from metal-metal hopping is independent of momentum and these bands remain completely flat.

Particle-hole symmetry is broken for $t_M \neq 0$. As $t_M > 0$ increases, the anti-bonding dispersive bands narrow until they become degenerate with the kagome-like flat band (for $t_M = t/2$), before widening again, but now at lower energy than the anti-bonding kagome-like flat band – indicating that the sign of the effective hopping integral for the anti-bonding bands changes at $t_M = t/2$. The bonding dispersive bands are widened by positive t_M . $t_M > 0$ also increases Δ_e and decreases Δ_h (Fig. 3b). For negative t_M these trends are reversed.

Thus, the five FTBs remain completely dispersionless, regardless of the values of δ and t_M , Fig. 3a-c. This is important because the values for δ and t_M in CPs and MOFs can vary dramatically, even between closely related materials [40].

In the CP and MOF literature, direct ligand-ligand hopping is often assumed to be negligible compared to the metal-ligand hopping. However, some counter examples are known [17, 41] and, we show below, that these terms have important qualitative effects on the band structure of the kagome-Lieb lattice. There are two near neighbor hoppings on the kagome-Lieb lattice: one across a triangle, t_{LT} , and another across a hexagon, t_{LH} ; Fig. 1a.

For $t_{LT} \neq 0$, $t_{LH} = 0$, two of the non-bonding bands develop a weak dispersion, (Fig. 3d), and the energy of the remaining exactly flat non-bonding band shifts to $E_{n_1} = t_{LT}$. The two kagome-like FTBs also remain flat. We can understand why these bands remain flat by ex-

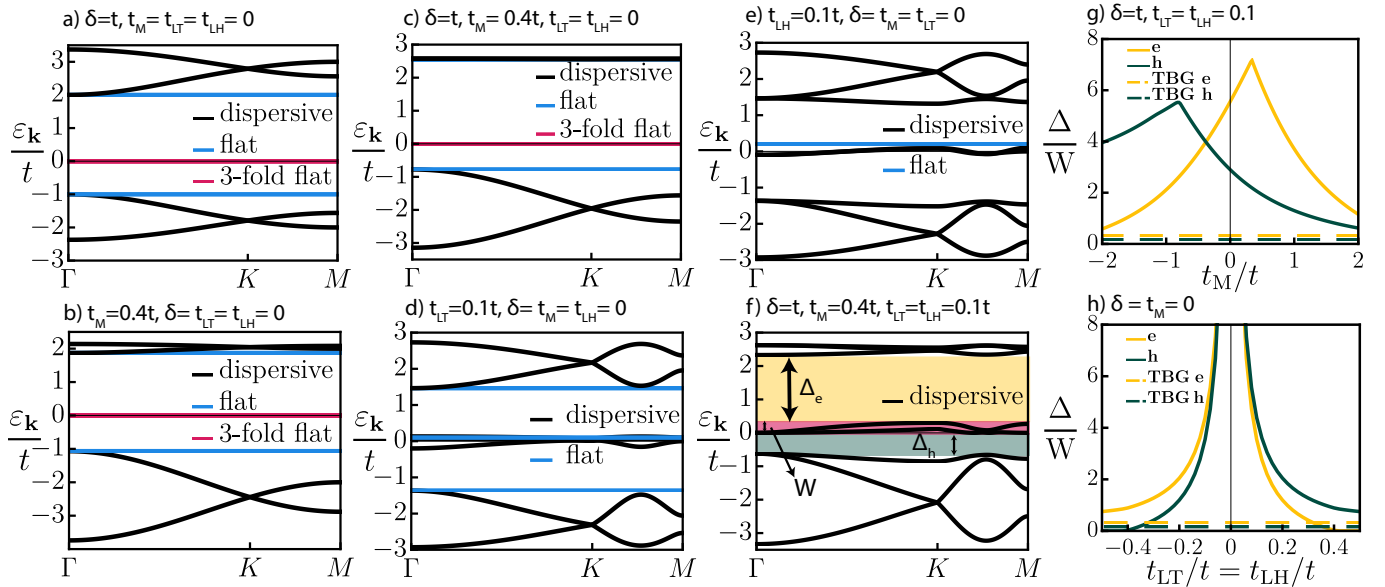


Fig. 3. Evolution of the band structure of the kagome-Lieb lattice tight-binding model with hopping beyond nearest neighbors. Five bands remain exactly flat even when (a) metal-ligand orbital energy differences, δ , (b) direct metal-metal hopping, t_M , or (c) both are included. (d) Ligand-ligand hopping across triangles, t_{LT} , leaves three exactly flat bands. (e) Ligand-ligand hopping across hexagons, t_{LH} , leaves one flat band. (f) Including all of these terms leaves no bands exactly flat, but the non-bonding bands remain gapped and narrow. The bandwidth of the non-bonding bands (W), the electron bandgap (Δ_e) and the hole bandgap (Δ_h) are labeled. (g,h) For a wide range of parameters, even for unfeasibly large t_M, t_{LT} and t_{LH} , the non-bonding bands remain much flatter and more isolated than the nearly-flat bands in TBG (from Ref. 5).

examining their localized wavefunctions, Fig. 2a-c. First consider the model with $t_{LT} \neq 0$ and all other parameters set to zero. The model now consists of disconnected triangles of ligand sites. A single triangle has a bonding orbital with energy $-2t_{LT}$, and two antibonding orbitals of energy t_{LT} [42]. $|n_1\rangle_h$ is a linear superposition of these triangular antibonding orbitals on six triangles, therefore it is an eigenstate with energy t_{LT} . We have seen above that $|n_1\rangle_h$ is a zero energy eigenstate of the terms proportional to t , δ , and t_m . Therefore, $|n_1\rangle_h$ is an eigenstate of the full model with $t_{LH} = 0$ with energy t_{LT} . A similar argument explains why $|+\rangle_h$ and $|-\rangle_h$, which can be viewed as superpositions of the triangular antibonding states and atomic metal states, are eigenstates. $|n_2\rangle_h$ and $|n_3\rangle_h$ are no longer eigenstates, as ligand-ligand hopping across a triangle results in a non-zero amplitudes on sites where the wavefunctions previously vanished, Fig. 2d,e.

For $t_{LT} = 0$, $t_{LH} \neq 0$, only one of the non-bonding bands remains exactly flat, with an energy of $E_{n_3} = 2t_{LH}$, Fig. 3e. This can be readily understood, as the model with $t_{LH} \neq 0$ and all other parameters set to zero consists of disconnected hexagons connecting ligand sites; and $|n_3\rangle_h$ is highest energy antibonding state of the tight-binding model on a single hexagon, Fig. 2e [43]. The other four localized states are not eigenstates for $t_{LH} \neq 0$, Fig. 2a-d.

For $t_{LT} \neq 0$, $t_{LH} \neq 0$, no completely flat bands remain, Fig. 3f. However, the non-bonding bands remain nearly flat and widely gapped, indeed, significantly flatter and more isolated than the nearly flat bands in TBG. The

relevant figures of merit are Δ_e/W and Δ_h/W , where W is the bandwidth of the non-bonding bands, which we plot in Fig. 3g,h. Clearly, for a wide range of parameters (even with metal-metal and ligand-ligand hopping much larger than expected) the non-bonding bands on the kagome-Lieb lattice are much flatter and more isolated than the nearly flat bands in TBG.

The large unit cells of CPs, MOFs, and COFs mean that longer range hopping is likely to be entirely negligible. Thus we expect that these conclusions will hold in any framework material that is well described by kagome-Lieb lattice tight-binding model. Electronic correlations, which are neglected here, will further flatten the non-bonding bands.

In Cu-BHT, there are multiple ligand orbitals near the Fermi energy, which makes the band structure somewhat more complex than the simple model considered here. Nevertheless, clear evidence for flat bands remains in DFT calculations for Cu-BHT. Furthermore, the enormous structural and chemical flexibility of CPs, MOFs, and COFs make these systems extremely well-suited to more precisely realizing the model described above.

Overall, owing to the very narrow, isolated bands at half-filling, materials with the kagome-Lieb lattice structure can be expected to display exotic, strongly correlated phenomena, including the potential for high-temperature superconductivity. The kagome-Lieb lattice has a significant advantage over other structures hosting FTBs, such as the kagome [37], Lieb [38], pyrochlore [37], and star [39] lattices: in these models, topology requires

zero bandgap between the flat band and dispersive bands, allowing excitations at arbitrarily low energies. This requirement is absent for the three non-bonding FTBs of the kagome-Lieb lattice. This allows large gaps between the nearly-flat bands and strongly dispersive bands, even when long-range hopping is included in the model. Nevertheless, a key design principle, identified here, is to

choose ligands with low direct ligand-ligand overlap as this minimizes the bandwidth of the non-bonding bands.

This work was supported by the Australian Research Council (DP180101483) and MEXT Quantum Leap Flagship Program (MEXT Q-LEAP) Grant Number JP-MXS0118069605.

-
- [1] L. Balents, C. R. Dean, D. K. Efetov, and A. F. Young, *Nat. Phys.* **16**, 725 (2020).
- [2] P. Törmä, S. Peotta, and B. A. Bernevig, *Nat. Rev. Phys.* **4**, 528 (2022).
- [3] Y. Cao, V. Fatemi, S. Fang, K. Watanabe, T. Taniguchi, E. Kaxiras, and P. Jarillo-Herrero, *Nature* **556**, 43 (2018).
- [4] Y. Cao, V. Fatemi, A. Demir, S. Fang, S. L. Tomarken, J. Y. Luo, J. D. Sanchez-Yamagishi, K. Watanabe, T. Taniguchi, E. Kaxiras, R. C. Ashoori, and P. Jarillo-Herrero, *Nature* **556**, 80 (2018).
- [5] S. Pathak, T. Rakib, R. Hou, A. Nevidomskyy, E. Ertekin, H. T. Johnson, and L. K. Wagner, *Phys. Rev. B* **105** (2022).
- [6] P. A. Lee, N. Nagaosa, and X.-G. Wen, *Rev. Mod. Phys.* **78**, 17 (2006).
- [7] B. J. Powell and R. H. McKenzie, *J. Phys. Condens. Matter* **18**, R827 (2006).
- [8] N. P. Ong and R. J. Cava, *Science* **305**, 52 (2004).
- [9] B. J. Powell, J. Merino, and R. H. McKenzie, *Phys. Rev. B* **80**, 085113 (2009).
- [10] Y. L. A. Pustogow, A. Chronister, Y.-S. Su, D. A. Sokolov, F. Jerzembeck, A. P. Mackenzie, C. W. Hicks, N. Kikugawa, S. Raghu, E. D. Bauer, and S. E. Brown, *Nature* **574**, 72 (2019).
- [11] Q. Si, R. Yu, and E. Abrahams, *Nat. Rev. Mater.* **1**, 16017 (2016).
- [12] S. Paschen and Q. Si, *Nat. Rev. Phys.* **3**, 9 (2021).
- [13] L. Sun, M. G. Campbell, and M. Dincă, *Angew. Chem. Int. Ed.* **55**, 3566 (2016).
- [14] M. B. Solomon, T. L. Church, and D. M. D'Alessandro, *CrystEngComm* **19**, 4049 (2017).
- [15] K. Geng, T. He, R. Liu, S. Dalapati, K. T. Tan, Z. Li, S. Tao, Y. Gong, Q. Jiang, and D. Jiang, *Chem. Rev.* **120**, 8814 (2020).
- [16] R. Murase, T. A. Hudson, T. S. Aldershof, K. V. Nguyen, J. G. Gluschke, E. P. Kenny, X. Zhou, T. Wang, M. P. van Koevorden, B. J. Powell, A. P. Micolich, B. F. Abrahams, and D. M. D'Alessandro, *J. Am. Chem. Soc.* **144**, 13242 (2022).
- [17] D. Kumar, J. Hellerstedt, B. Field, B. Lowe, Y. Yin, N. V. Medhekar, and A. Schiffrin, *Adv. Funct. Mater.* **31**, 2106474 (2021).
- [18] H. L. Nourse, R. H. McKenzie, and B. J. Powell, *Phys. Rev. B* **103**, L081114 (2021).
- [19] H. L. Nourse, R. H. McKenzie, and B. J. Powell, *Phys. Rev. B* **104**, 075104 (2021).
- [20] H. L. Nourse, R. H. McKenzie, and B. J. Powell, *Phys. Rev. B* **105**, 205119 (2022).
- [21] J. Merino, M. F. López, and B. J. Powell, *Phys. Rev. B* **103**, 094517 (2021).
- [22] X. Zhang, Y. Zhou, B. Cui, M. Zhao, and F. Liu, *Nano Lett.* **17**, 6166 (2017).
- [23] X. Huang, S. Zhang, L. Liu, L. Yu, G. Chen, W. Xu, and D. Zhu, *Angew. Chem. Int. Ed.* **57**, 146 (2018).
- [24] T. Takenaka, K. Ishihara, M. Roppongi, Y. Miao, Y. Mizukami, T. Makita, J. Tsurumi, S. Watanabe, J. Takeya, M. Yamashita, K. Torizuka, Y. Uwatoko, T. Sasaki, X. Huang, W. Xu, D. Zhu, N. Su, J.-G. Cheng, T. Shibauchi, and K. Hashimoto, *Sci. Adv.* **7** (2021).
- [25] N. Regnault, Y. Xu, M.-R. Li, D.-S. Ma, M. Jovanovic, A. Yazdani, S. S. P. Parkin, C. Felser, L. M. Schoop, N. P. Ong, R. J. Cava, L. Elcoro, Z.-D. Song, and B. A. Bernevig, *Nature* **603**, 824 (2022).
- [26] M. J. Kalmutzki, N. Hanikel, and O. M. Yaghi, *Sci. Adv.* **4**, eaat9180 (2018).
- [27] R. Robson, *J. Chem. Soc., Dalton Trans.* **2000**, 3735 (2000).
- [28] R. Robson, *Dalton Trans.* **2008**, 5113 (2008).
- [29] O. M. Yaghi, M. O'Keeffe, N. W. Ockwig, H. K. Chae, M. Eddaoudi, and J. Kim, *Nature* **423**, 705–714 (2003).
- [30] H. Furukawa, K. E. Cordova, M. O'Keeffe, and O. M. Yaghi, *Science* **341**, 1230444 (2013).
- [31] M. S. Lohse and T. Bein, *Adv. Funct. Mater.* **28**, 1705553 (2018).
- [32] B. Cui, X. Zheng, J. Wang, D. Liu, S. Xie, and B. Huang, *Nat. Commun.* **11**, 66 (2020).
- [33] M. Hua, B. Xia, M. Wang, E. Li, J. Liu, T. Wu, Y. Wang, R. Li, H. Ding, J. Hu, Y. Wang, J. Zhu, H. Xu, W. Zhao, and N. Lin, *J. Phys. Chem. Lett.* **12**, 3733 (2021).
- [34] R. Dong, Z. Zhang, D. C. Tranca, S. Zhou, M. Wang, P. Adler, Z. Liao, F. Liu, Y. Sun, W. Shi, Z. Zhang, E. Zschech, S. C. B. Mannsfeld, C. Felser, and X. Feng, *Nat. Commun.* **9**, 2637 (2018).
- [35] J.-H. Dou, L. Sun, Y. Ge, W. Li, C. H. Hendon, J. Li, S. Gul, J. Yano, E. A. Stach, and M. Dincă, *J. Am. Chem. Soc.* **139**, 13608 (2017).
- [36] B. Sutherland, *Phys. Rev. B* **34**, 5208 (1986).
- [37] D. L. Bergman, C. Wu, and L. Balents, *Phys. Rev. B Condens. Matter Mater. Phys.* **78** (2008).
- [38] Y. Hwang, J.-W. Rhim, and B.-J. Yang, *Phys. Rev. B* **104**, 085144 (2021).
- [39] A. C. Jacko, C. Janani, K. Koepernik, and B. J. Powell, *Phys. Rev. B* **91**, 125140 (2015).
- [40] E. P. Kenny, A. C. Jacko, and B. J. Powell, *Inorg. Chem.* **60**, 11907 (2021).
- [41] M. Fuchs, P. Liu, T. Schwemmer, G. Sangiovanni, R. Thomale, C. Franchini, and D. D. Sante, *J. Phys.: Mater.* **3**, 025001 (2020).
- [42] J. Merino, B. J. Powell, and R. H. McKenzie, *Phys. Rev. B* **73**, 235107 (2006).
- [43] J. Lowe, *Quantum Chemistry* (Elsevier, London, 2012).